Time-dependent mobility and recombination of the photoinduced charge carriers in conjugated polymer/fullerene bulk heterojunction solar cells

A. J. Mozer,* G. Dennler, and N. S. Sariciftci
Linz Institute for Organic Solar Cells (LIOS,) Johannes Kepler University, Linz, Austria

M. Westerling, A. Pivrikas, and R. Österbacka
Department of Physics, Åbo Akademi University, Turku, Finland

G. Juška
Department of Solid State Electronics, Vilnius University, Lithuania
(Received 23 February 2005; revised manuscript received 6 May 2005; published 20 July 2005)

Time-dependent mobility and recombination in the blend of poly[2-methoxy-5-(3,7-dimethyloctyloxy)-phenylene vinylene] (MDMO-PPV) and 1-(3-methoxycarbonyl)propyl-1-phenyl-(6,6)-C_{61}(PCBM) is studied simultaneously using the photoinduced charge carrier extraction by linearly increasing voltage technique. The charge carriers are photogenerated by a strongly absorbed, 3 ns laser flash, and extracted by the application of a reverse bias voltage pulse after an adjustable delay time (t_{del}). It is found that the mobility of the extracted charge carriers decreases with increasing delay time, especially shortly after photoexcitation. The time-dependent mobility $\mu(t)$ is attributed to the energy relaxation of the charge carriers towards the tail states of the density of states distribution. A model based on a dispersive bimolecular recombination is formulated, which properly describes the concentration decay of the extracted charge carriers at all measured temperatures and concentrations. The calculated bimolecular recombination coefficient $\beta(t)$ is also found to be time-dependent exhibiting a power law dependence as $\beta(t)=\beta_0 t^{-(1-\gamma)}$ with increasing slope $(1-\gamma)$ with decreasing temperatures. The temperature dependence study reveals that both the mobility and recombination of the photogenerated charge carriers are thermally activated processes with activation energy in the range of 0.1 eV. Finally, the direct comparison of $\mu(t)$ and $\beta(t)$ shows that the recombination of the long-lived charge carriers is controlled by diffusion.

DOI: 10.1103/PhysRevB.72.035217 PACS number(s): 72.20.Jv, 72.40+w, 72.80.Le, 72.80.Rj

I. INTRODUCTION

The investigation of the charge carrier recombination kinetics in noncrystalline organic materials is of fundamental importance from a material characterization point of view, as well as due to the application of these materials in optoelectronic devices, such as photodetectors, solar cells,[1] and light emitting diodes.[2] Particularly, the charge generation[3] and recombination[4] mechanism within the interpenetrating network of electron donating conjugated semiconducting polymers and electron accepting fullerenes is the focus of current interest.[5] Photoexcitation of the conjugated polymer in the blend of poly[2-methoxy-5-(3,7-dimethyloctyloxy)-phenylene vinglene] (MDMO-PPV) and 1-(3-methoxycarbonyl)propyl-1-phenyl-(6,6)-C_{61} (PCBM) results in a rapid electron transfer[6] from MDMO-PPV to PCBM, leaving a positive radical cation (polaron) on the polymer backbone and a radical anion on the fullerene molecule. The charge-separated configuration is relatively long lived (lifetime of the order of μs-ms), which is a prerequisite for fabrication of efficient photovoltaic devices (bulk heterojunction solar cells).[7]

Several optical techniques, including light induced electron spin resonance (LESR),[8] photoinduced absorption (PIA),[9] photoinduced reflection-/absorption (PIRA),[10] transient absorption (TA),[4,11] and more recently, a flash photolysis time-resolved microwave conductivity technique (FP-TRMC) (Ref. 12) has been used to study the recombination of the photoinduced charge carriers at various time scales and temperatures. The TA studies, in which the change in the transmission of the sample [represented as the change of the optical density (ΔOD)] upon photoexcitation is monitored in a time resolved experiment, identified a faster ($\leqslant$400 ns) and a slower (μs-ms) component of the recombination dynamics of the photogenerated polarons in the MDMO-PPV/PCBM blend. The latter, slower phase of the recombination follows a power law decay as $\Delta\mathrm{OD} \propto t^{-\lambda}, \lambda=0.4$ at room temperature. Moreover, the ΔOD signal saturates above a light intensity of $\sim 1\ \mu\mathrm{J/cm^2/pulse}$. The initial fast light-intensity-dependent component was attributed to recombination of charges prior trapping (above the mobility edge),[13] meanwhile the slow, dispersive recombination is controlled by diffusion limited recombinations of holes localized below the mobility edge with PCBM anions. The LESR study of Schultz *et al.*, on the other hand, showed that there are persistent charge carriers in such blends with lifetimes up to hours at 4 K and a temperature-independent tunneling-based recombination process was proposed.[8]

In this paper, we applied the photoinduced charge carrier extraction by linearly increasing voltage technique (photo-CELIV) to study the mobility and recombination of the charge carriers at μs-ms time scale. This technique allows us to determine the mobility and the lifetime of the charge carriers simultaneously. The question of particular interest is

whether the long-lived charges are mobile enough to be collected at external electrodes, or rather, they are localized deeply within a manifold of trap states, and will be lost for charge collection in photodiodes and solar cells.

We have recently observed that the mobility depends on the applied time delay between the photogeneration and the charge collection especially shortly after photoexcitation.[14] The temperature dependence studies presented herein confirm that the observed time-dependent mobility is due to relaxation of the charge carriers towards the tail states of the density of states distribution. Moreover, in good agreement with previous works, [15,16] we show that the recombination dynamics within the μs-ms is primarily controlled by diffusion of the charge carriers in the bulk rather than by interfacial processes associated with phase segregation of the blend. Finally, the simultaneous determination of mobility and the lifetime of the charge carriers suggest that the majority of the long-lived charge carriers can be collected in typical bulk heterojunction solar cells at short circuit conditions.

II. EXPERIMENTAL

A. Photo-CELIV technique

The schematic response of the photo-CELIV [14,17] is shown in Fig. 1. The sample consists of a thin (200–350 nm) layer of MDMO-PPV:PCBM sandwiched between a transparent ITO-coated glass and evaporated aluminum electrodes, which structure is typical of a bulk heterojunction solar cell. Upon application of a reverse bias triangular-shaped voltage pulse with a voltage rise speed $A=dU/dt$, the typical electrical response is a rectangular-shaped current transient with a plateau value corresponding to the capacitive displacement current $j(0)=A\times\varepsilon\varepsilon_0/d$, where $\varepsilon,\varepsilon_0$ is the dielectric constant of the material and vacuum, respectively, and d is the thickness of the dielectric. When a strongly absorbed laser flash hits the sample, charge carriers are photogenerated throughout the layer. The photogenerated charge carriers either undergo recombination or exit the device through the external circuit under the influence of the built-in electric field (short circuit condition). The external photocurrent upon photoexcitation can be minimized by the application of a dc offset bias (U_{offset}) forcing the charge carriers to remain in the device and to recombine. The remaining charge carriers can be extracted after an adjustable delay time (t_{del}). By selecting the proper voltage rise speed A, the extraction current reaches a maximum value Δj as shown by the dashed line in Fig. 1, and from the time to reach the current maximum t_{max}, the mobility μ can be calculated according to Eq. (1):

$$\mu=\frac{2d^2}{3At_{\text{max}}^2\left[1+0.36\frac{\Delta j}{j(0)}\right]}\quad\text{if }\Delta j\leqslant j(0). \tag{1}$$

Equation (1) has been derived by solving the continuity, current, and Poisson equations.[18] The expression $1+0.36\Delta j/j(0)$ in the denominator of Eq. (1) has been introduced to compensate for the redistribution of the electric field during charge extraction, and it is valid for moderately conductive samples, i.e., when the number of extracted charge carriers equals or is less than the capacitive charge $\Delta j\leqslant j(0)$.[19]

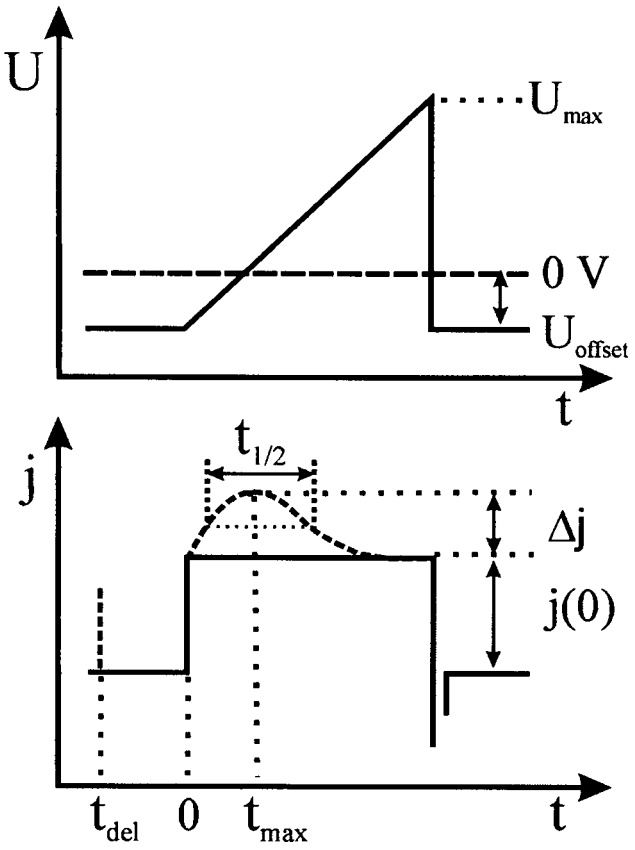

FIG. 1. Schematic illustration of the photo-CELIV method. U is the applied voltage to the sample, j is the corresponding current transient. The full line (dashed line) corresponds to the extraction transient in the dark (upon a short laser flash). The measurement parameters $j(0),\Delta j,t_{\text{del}},t_{\text{max}},U_{\text{max}}$, and U_{offset} are introduced in Sec. II A and $t_{1/2}$ is introduced in Sec. IV A.

B. Sample preparation and experimental details

The thin organic films were deposited from chlorobenzene solutions (0.5 mg polymer/1 ml solvent) of MDMO-PPV:PCBM 1:4 by weight using the spin coating technique on prestructured ITO-coated glass. Aluminum as top electrode was deposited by thermal evaporation defining a device area of 3 to 5 mm^2. The devices were placed in a liquid-nitrogen-cooled vacuum-loaded cryostat and illuminated from the ITO side by 3 ns pulses of a Nd:YAG laser at 532 nm excitation wavelength (Coherent Infinity 40-100). The reverse bias triangular-shaped voltage pulse (ITO connected as the negative terminal) was applied by a digital function generator (Stanford Research DS 345), and the time delay between the light pulse and the voltage pulse was adjusted by a digital delay generator (Stanford Research DG 535). The light intensity incident on the sample was measured by a pyroelectric detector (Ophir PE25-S), and was varied using a set of optical density (OD) filters. The laser pulse was monitored using a biased silicon detector (Newport 818-BB-20).

The photo-CELIV transients were recorded by a digital storage oscilloscope (Tektronix TDS754C) using variable load resistance. The MDMO-PPV was synthesized by the group of Vanderzande according Ref. 20, and PCBM was purchased from J. C. Hummelen (Rijksuniversiteit Groningen, The Netherlands).

III. THEORY OF DISPERSIVE RECOMBINATION DYNAMICS

The recombination of long-lived charge carriers in conjugated polymers is usually described as a nongeminate bimolecular recombination process.[21] In addition to simple bimolecular recombination, a complete description of the recombination dynamics should include the effects of structural disorder, i.e., variations in the positions and local orientations of the polymer chains and energetic disorder attributed to the distribution of conjugation lengths and differences in the local environment. These static properties of the material give rise to a distribution of localized states (DOS). Charge carrier hopping within the DOS is proposed as an adequate model for describing transport in disordered organic materials.[22–25] Charge carriers created randomly within the DOS execute random walks in the course of which they relax towards the tail states of the DOS. During this thermalization process the time derivative of the mean-square displacement of the charge carriers becomes time dependent, known as the dispersive regime. Consequently, the diffusion coefficient D of the charge carriers becomes time dependent and decreases during the relaxation process. In the long-time regime when the charge carriers have relaxed and filled up the tail states, a dynamic equilibrium is attained in the case of a Gaussian DOS. In this nondispersive regime the charge migration is governed by thermally assisted jumps and the diffusion coefficient adopts a constant value D_∞.[26]

According to Smoluchowski's theory of diffusion-controlled bimolecular reactions, the bimolecular recombination coefficient (β) is proportional to the sum of the charge carrier diffusion coefficients ($D=D_n+D_p$), their interaction radius (R), and the fraction (f) of charges annihilated after an encounter:[27–29]

$$\beta = 4\pi f R D. \tag{2}$$

Since the diffusion coefficient D is time dependent during thermalization, the bimolecular rate coefficient will also become time dependent, i.e., $\beta(t)=4\pi fRD(t)$, which has been confirmed using Monte Carlo simulation techniques.[30] Assuming a bimolecular recombination equation with a time-dependent rate coefficient $\beta(t)$ we write

$$\frac{dn}{dt} = \frac{dp}{dt} = -\beta(t) n p, \tag{3}$$

where n,p is the concentration of electrons and holes, respectively. Assuming charge neutrality, i.e., $n=p$, the solutions for $n(t)$ and $p(t)$ are given by

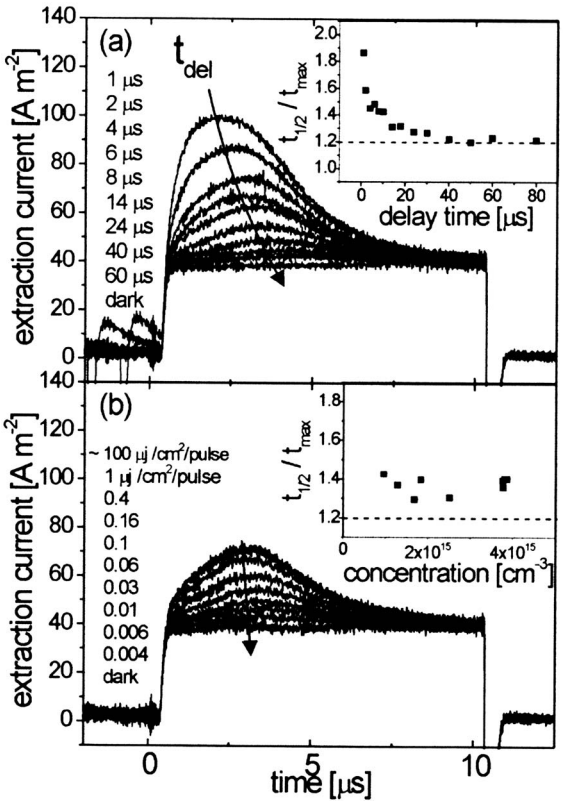

FIG. 2. Photo-CELIV transients recorded at 300 K at (a) various delay times at fixed light intensity; (b) varying illumination intensities attenuated using optical density filters at fixed 5 μs delay time. The voltage rise speed A was 4 V/10 μs. The insets show the calculated dispersion parameters $t_{1/2}$ to t_{max} versus delay time and the concentration of the extracted charge carriers, respectively.

$$n(t) = p(t) = \frac{n(0)}{1 + n(0)\int_0^t \beta(t)dt}, \tag{4}$$

where $n(0)=p(0)$ is the initial ($t=0$) concentration of photogenerated charge carriers. The exact functional time dependence of $D(t)$ [and thus of $\beta(t)$] in the dispersive regime is strongly dependent on the form of the DOS distribution. In the case of hopping in an exponential DOS, or equivalently, multiple trapping, the diffusion coefficient exhibits a power-law time dependence,[31] i.e., $D(t)\sim t^{-\alpha}$ whereas for a Gaussian DOS it is not trivial to cast $D(t)$ into an explicit analytical expression for all times.[26,30] However, in the case of a Gaussian DOS $D(t)$ can still be approximated by a power-law function within a limited time interval.

IV. RESULTS

A. Delay-time dependence of the mobility

Figure 2 shows the recorded photo-CELIV curves at 300 K at various (a) delay times and (b) incident light intensity varied by OD filters at fixed (5 μs) delay time. The U_{offset} was −0.7 V, which is very close to the built-in electric field of the devices as indicated by the negligible photocurrent

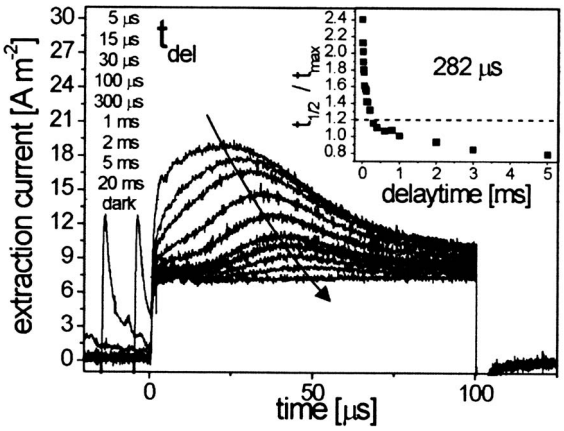

FIG. 3. Photo-CELIV transients recorded at 150 K at various delay times. The voltage rise speed A was 8 V/100 μs. The inset shows the dispersion parameter $t_{1/2}$ to $t_{\max}$ versus the delay time. The time to reach the ideal nondispersive value is also displayed.

immediately upon photoexcitation. The maximum of the extraction current (Δj) decreases with increasing delay time, which is related to the recombination of the photogenerated charge carriers. Moreover, the time when the extraction current reaches its maximum ($t_{\max}$) shifts to longer times, which is related to decreasing mobility according to Eq. (1). Interestingly, the $t_{\max}$ remains almost constant when the light intensity is decreased at a fixed delay time [Fig. 2(b)], and the number of extracted charge carriers saturates with increasing light intensity above ~ 1 μJ/pulse/cm^2.

Dispersion of the photo-CELIV transients (how fast it rises and decays before it reaches its maximum value) can be characterized by $t_{1/2}$ to $t_{\max}$ as it is illustrated schematically in Fig. 1. The calculated value for an ideal nondispersive transient is 1.2.[32] The recorded photo-CELIV transients shown in Fig. 2(a) are dispersive at short delay times as indicated by the $t_{1/2}$ *to* $t_{\max}$ ratios well above 1.2, which gradually decreases to the ideal nondispersive value of 1.2 at longer time delays [inset of Fig. 2(a)]. An interesting feature is the sublinear slope of the initial current rise (dj/dt) at short delay times, which is related to a time-dependent mobility during extraction.[19] On the contrary, the $t_{1/2}$ *to* $t_{\max}$ values do not change significantly by varying the light intensity (charge carrier concentration) indicating a concentration independent but time-dependent dispersion at short delay times. Moreover, the majority of the photogenerated charge carriers can be extracted by the extraction pulse at all delay times as shown by the end of the pulse extraction current, which indicates that trapping into deep traps at this time scale is negligible.

The photo-CELIV curves recorded at various delay times at 150 K are shown in Fig. 3. Similarly to the room temperature transients, the $t_{\max}$ shifts to longer times accompanied by a gradually decreasing dispersion as $t_{\rm del}$ is increased. However, the time to reach the ideal nondispersive value of 1.2 takes approximately one order of magnitude longer at 150 K. An interesting feature is that the dispersion parameter decreases even below the ideal value of 1.2, which is attributed to the electric field dependence of the mobility. The more

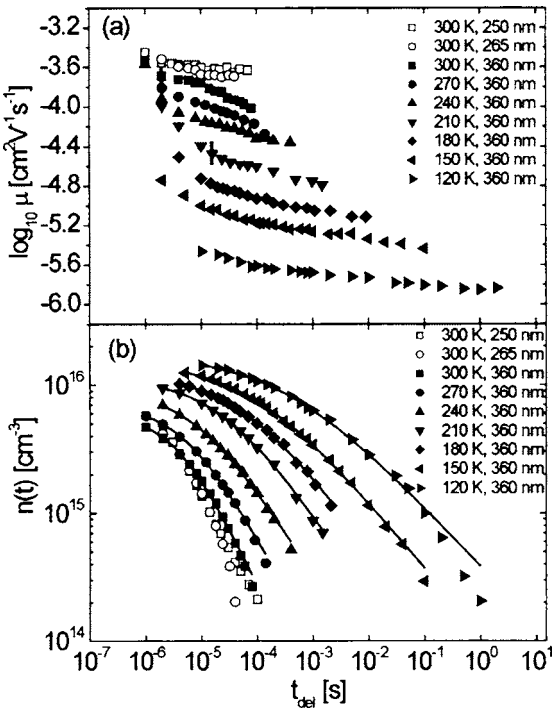

FIG. 4. (a) and (b) Mobility values and the concentration of extracted charge carriers versus the delay time for samples with different active layer thickness, respectively. The mobility and concentration values measured for the 360 nm device at various temperatures are also displayed.

pronounced electric field dependence of the mobility at these lower temperatures and longer delay times can be also identified from the superlinear initial current rise (dj/dt) of the transients.[19] An important difference is that the end of the extraction current does not reach the capacitive step value $j(0)$ within the applied time window, which shows that some portion of the charge carriers are trapped on the time scale of the photo-CELIV extraction at lower temperatures.

The mobility values calculated according to Eq. (1) are plotted versus delay time in Fig. 4(a). Results for devices with different active layer thickness are shown for comparison, and the temperature dependence of the mobility for the device with 360 nm active layer thickness is shown. The mobility clearly decreases with increasing delay time at every temperature, and also exhibits pronounced temperature dependence. Two different slopes in the $\log_{10}\mu$ versus $\log_{10} t$ can be identified as indicated by the appearance of a "kink" at shorter time delays (as indicated by the solid lines at 300 and 210 K). The "kink" shifts to longer times at lower temperatures. The mobility values at the shortest delay times correspond well between samples with different thickness, yet the mobility values determined at longer time delays (and correspondingly, the slope of the $\log_{10}\mu$ versus $\log_{10} t$ plots after the kink) appear to vary with the sample thickness. Photo-CELIV transient versus various delay times have also been recorded by illuminating the samples from the aluminum side. Although generally fewer carriers are extracted due to light attenuation by the aluminum electrode, the time dependence of the mobility was very similar as shown in Fig. 4(a). Moreover, photo-CELIV transients were recorded using

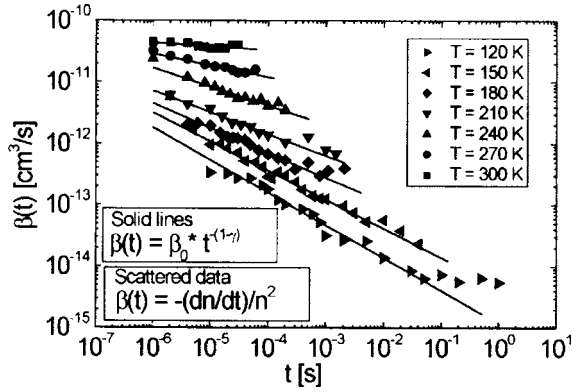

FIG. 5. Bimolecular recombination coefficient calculated using Eq. (3) (scattered data), and obtained by fitting the concentration decay using Eq. (5) (solid lines) versus delay time at various temperatures.

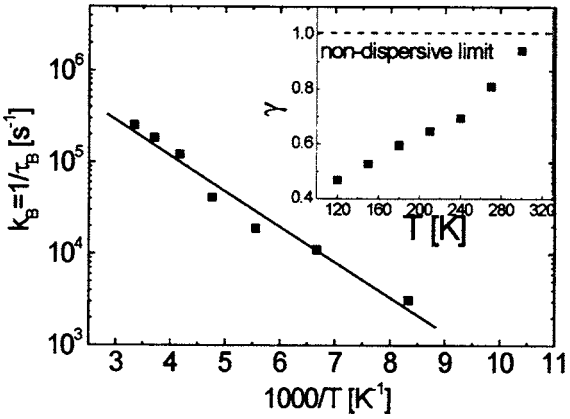

FIG. 6. Arrhenius plot of the "effective" bimolecular recombination rate of Eq. (5). The inset shows the temperature dependence of the dispersion parameter γ.

355 nm as the excitation wavelength, at which the optical density of the films is approximately twice as large as compared to at 532 nm. Nevertheless, the calculated mobility values and its time dependence were nearly identical using either excitation wavelength.

In Fig. 4(b), the concentration of extracted charge carriers calculated by integrating the photo-CELIV transients is plotted versus the delay time. The concentration decay for samples with different active layer thickness is also displayed. Using the time dependent bimolecular recombination equation [Eq. (3)], $\beta(t)$ is calculated, and shown as scattered data in a double logarithmic plot in Fig. 5. The data reveals power-law time dependence for $\beta(t)$ for all temperatures. The power-law slope has the value 0.06 at 300 K and gradually increases at lower temperatures reaching the value 0.53 at 120 K. Thus, for all temperatures between 120 and 300 K, the time-dependent bimolecular recombination coefficient can be described as $\beta(t)=\beta_0 t^{-(1-\gamma)}$, where β_0 and γ are temperature-dependent parameters. Using this functional form of $\beta(t)$ the integral in Eq. (4) can be evaluated yielding

$$n(t) = p(t) = \frac{n(0)}{1 + (t/\tau_B)^{\gamma}}, \tag{5}$$

where $\tau_B=\{\gamma/[n(0)\beta_0]\}^{1/\gamma}$ is an "effective" bimolecular lifetime. The fits to the decay data using Eq. (5) are shown as solid lines in Fig. 4(b), and the resulting $\beta(t)$ calculated from the fit parameters β_0 and γ is shown for each temperature as solid lines in Fig. 5 in good agreement with the scattered data except at 120 K, when the recombination of the long-lived charges tends to deviate.

The "effective" bimolecular lifetime τ_B obtained from the decay fits decreases with increasing temperature, being 4 μs at 300 K and 319 μs at 120 K. The temperature dependence of the "effective" bimolecular recombination rate $k_B=1/\tau_B$ is plotted in an Arrhenius plot in Fig. 6, clearly showing a thermally activated behavior. The solid line is a fit to $k_B=k_0\exp(-\Delta E/kT)$, yielding an activation energy of $\Delta E=77$ meV. The temperature dependence of the dispersion parameter γ is shown in the inset of Fig. 6, showing that γ increases monotonously with decreasing temperature. At 120 K the value of γ is 0.47, related to a highly dispersive (strongly time-dependent) recombination process, whereas at 300 K the value γ is 0.94 which is close to a nondispersive recombination ($\gamma=1$).

B. Concentration dependence of the mobility

It has been argued that the charge carrier mobility in disordered organic semiconductors may depend on the charge carrier concentration.[33–37] Tanase *et al.* have shown that the several orders of magnitude higher charge carrier mobility observed in field effect transistors as compared to light emitting diodes can originate from the increased charge carrier mobility at higher charge carrier densities, especially $>10^{16}$ cm^{-3}. Similarly, it was also demonstrated that the enhanced space-charge-limited current in poly(*p*-phenylene vinylene) diodes at higher applied voltages is due to the enhancement of the charge carrier mobility at higher charge carrier densities rather than the effect of the (positive) electric field dependence of mobility as previously assumed.[38] Arkhipov *et al.* argued, on the other hand, that the mobility may also decrease in disordered materials with increasing charge carrier concentration due to the effect of additional Coulomb traps introduced by charge carrier doping.[34,37]

The time-dependent mobility in Fig. 4(a), therefore, can originate from the concentration (occupational density) dependence of the mobility as argued above. In order to test the effect of charge carrier concentration, photo-CELIV curves at various light intensities at a fixed delay time has been recorded. Figure 7 shows the logarithm mobility versus the concentration of extracted charge carriers calculated from (a) light intensity-dependent measurements at fixed delay times (b) from delay time-dependent measurements at fixed light intensity ($\sim$100 μJ/cm^2/pulse). The mobility is slightly dependent on the concentration of extracted charge carriers at fixed delay time, with increasing slope at lower temperatures. The concentration dependence of mobility calculated at fixed light intensity but various delay times [Fig. 7(b)] correspond well to that of Fig. 7(a) at longer delay times, yet deviates significantly at shorter time delays. The comparison of Figs. 7(a) and 7(b) indicates that the time-dependent mo-

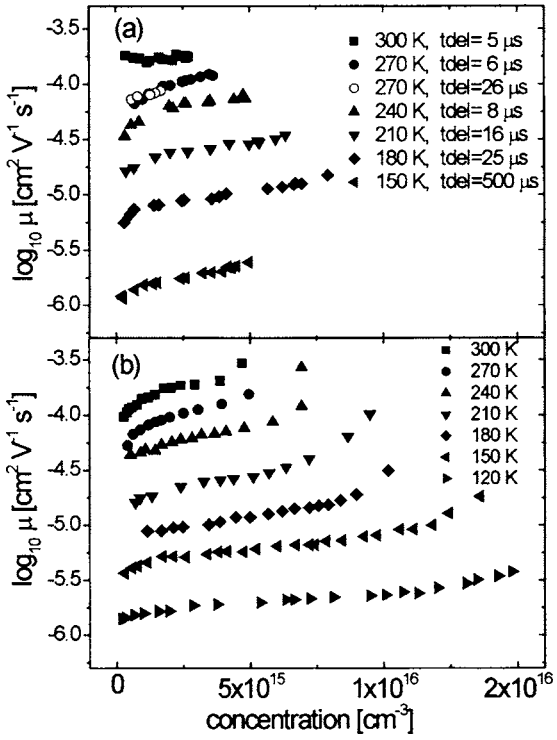

FIG. 7. Mobility versus the concentration of the extracted charge carriers calculated from (a) light intensity dependent measurements at fixed delay times; (b) delay time-dependent measurements at fixed light intensity. The delay time used during the light intensity dependent studies is displayed in the key.

bility in Fig. 4(a) especially at shorter delay times cannot be attributed to the concentration dependence of the mobility alone.

C. Applied voltage (electric-field) dependence of the mobility

Figure 8 shows the recorded photo-CELIV curves at various applied voltages (U_{max}) at fixed light intensity and fixed 15 μs delay time at room temperature. The t_{max} shifts to

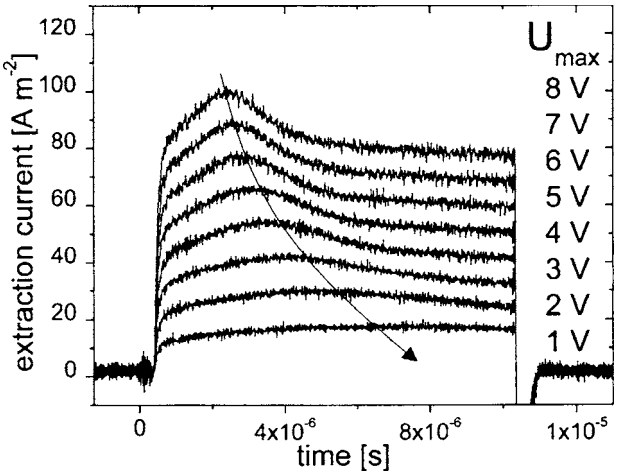

FIG. 8. Photo-CELIV transients recorded at 300 K by changing the maximum of the applied voltage pulse.

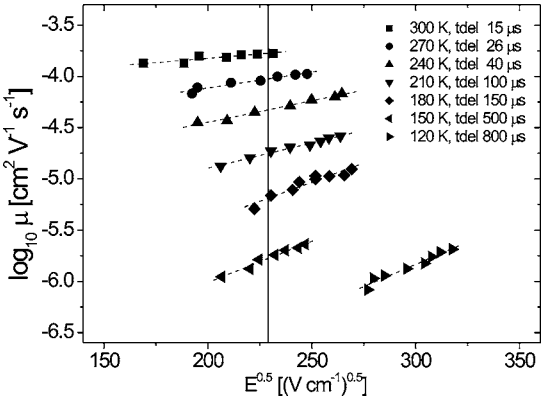

FIG. 9. Electric field dependence of the mobility determined at various temperatures. The solid vertical line corresponds to an electric field of 5.2×10^5 V cm^{-1}. The dashed lines represent linear fits of the data, and the applied delay times during the measurements are also displayed.

longer times as the maximum of the voltage pulse is decreased, which is related to the electric field dependence of the mean velocity of the charge carriers. The electric field during the photo-CELIV extraction varies constantly, and depends on both space and time coordinate. The electric field (E) can be calculated at the extraction maximum as[39]

$$E = \frac{A \times t_{max}}{d}. \tag{6}$$

Figure 9 shows the calculated mobility versus the square root of the electric field at various temperatures. A long delay time between the light pulse and the voltage pulse has been used for these voltage dependent measurements at every temperature as displayed in Fig. 9.

The field dependence of mobility follows a Poole-Frenkel-like dependence at all temperatures within the experimentally accessible electric-field range. The slope of the field dependence is increasing with decreasing temperature. The mobility values taken at a constant 5.2×10^5 V cm^{-1} electric field along the solid line are plotted versus $1000/T$ in Fig. 10, and a linear relationship is found. The apparent activation energy (ΔE_μ) of the mobility can be calculated from $\mu=\mu_0\exp(-\Delta E_\mu/kT)$, where μ_0 is a prefactor mobility and k is the Boltzmann constant. From the slope of the linear fit in Fig. 9, $\Delta E_\mu=120$ meV is calculated.

Alternatively, the temperature and electric field dependence of mobility can be analyzed within the framework of disorder formalism, which predicts a non-Arrhenius type activation of the mobility extrapolated to zero electric field [$\log_{10}\mu(E=0)\propto 1/T^2$] according to[23]

$$\mu(T,E) = \mu_0 \exp\left[-\frac{2}{3}\left(\frac{\sigma}{kT}\right)^2\right]\exp\left\{C\left[\left(\frac{\sigma}{kT}\right)^2 - \Sigma^2\right]E^{1/2}\right\}, \tag{7}$$

where σ [eV] is the width of the Gaussian density of states, Σ is a parameter characterizing positional disorder, μ_0 [cm^2 V^{-1} s^{-1}] is a prefactor mobility in the energetically

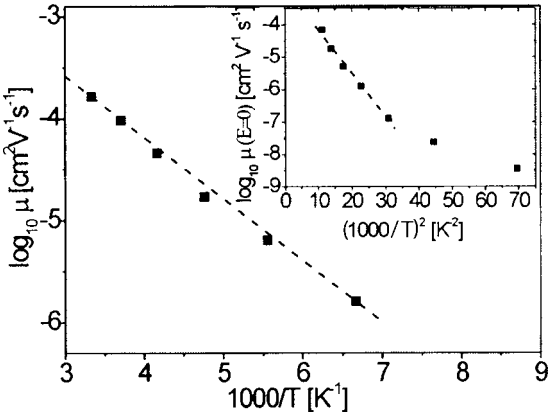

FIG. 10. Arrhenius plot of the mobility values take at a constant $E=5.2\times10^5$ V cm^{-1} electric field from Fig. 9. The inset shows the logarithm of mobility extrapolated to zero electric field versus $(1000/T)^2$.

disorder-free system E [V cm^{-1}] is the electric field and C is a fit parameter.

The $\log_{10}\mu(E=0)$ is plotted in the inset of Fig. 10 versus $(1000/T)^2$, and $\sigma=60$ meV is calculated from the higher temperature range. It is clearly seen that the measured temperature dependence deviates at lower temperatures from the prediction of Eq. (7).

V. DISCUSSION

A. Time-dependent mobility

The time dependence of the mean hopping rate of photoexcitations generated in nonequilibrium conditions appears to be intrinsic to disordered semiconductors in which the charge transport sites are subject to both energetic and spatial disorder.[40] Numerous theoretical studies employing Monte Carlo simulation techniques,[23] an effective medium approach[41] and recently, an analytical description[42] based on the transport level argument have been used to describe charge transport in the presence of both energetic and spatial disorder. Generally, the hopping rate between localized states is described by the Miller-Abrahams form[43]

$$\nu_{ij}=\nu_0\exp\left(-2\gamma a\frac{\Delta R_{ij}}{a}\right)\begin{cases}\exp\left(-\dfrac{\varepsilon_j-\varepsilon_i}{kT}\right), & \varepsilon_j>\varepsilon_i,\\ 1, & \varepsilon_j<\varepsilon_i,\end{cases} \tag{8}$$

where ν_{ij} is the hopping rate between site i and j with energy ε_i and ε_j, a is the average lattice distance. The first exponential in Eq. (8) describes the electronic wave function overlap, and the second describes a Boltzmann factor for sites upwards in energy. Equation (8) postulates that only charge carrier hops to sites higher in energy are thermally activated, therefore only these jumps are accelerated by the electric field. The rate for downward jumps is 1, which assumes that energy can always be dissipated rapidly via the large number of high frequency phonons typical for organic conjugated materials. Due to the asymmetric hopping rates, a dynamic equilibrium may be attained when the number of even lower lying sites is so low, that on average all the jumps will be thermally activated upward jumps. Arkhipov *et al.* have shown that in equilibrium the hopping process occurs between sites thermalized within the tail of the distribution of states at a statistically defined transport level, reducing the problem to a multiple trapping and release model in which the transport level is equivalent to a mobility edge.[13] Whether the mean velocity of the packet of migrating charge carriers generated under nonequilibrium conditions reaches a quasistatic value depends on the shape of the distribution of the localized states. In the case of a Gaussian DOS, the packet of photogenerated charges is expected to reach quasiequilibrium transport at longer times. The relaxation time increases as $t_{\mathrm{rel}}/t_0=10\exp[1.07\,(\sigma/kT)^2]$ (where t_0 is the dwell time of a carrier without disorder) with decreasing temperature.[23] Such relaxation process occurs simultaneously with charge extraction during the time-of-flight transient photocurrent method,[44] in which a sheet of photogenerated charge carriers drifts across the sample under a uniform, externally applied electric field. Since the time to reach quasiequilibrium increases stronger than the transit time with decreasing temperature, eventually charge transport without quasiequilibrium is probed leading to a frequently observed nondispersive to dispersive transition in transport.[45] The delay time between charge generation and extraction is varied using the photo-CELIV technique, which enables us to *separate* the energy equilibration process from the charge extraction.

A rapid relaxation of the charge carriers within the intrinsic DOS towards the tail states of the distribution towards quasiequlibrium is observed in Fig. 4(a) as the "kink" in the $\log_{10}\mu$ versus $\log_{10} t$ plot, with a relaxation time that increases strongly as the temperature is decreased. Further indication is given by the observed transition in the shape of the photo-CELIV transients from dispersive shortly after photoexcitation to nondispersive at longer time delays.

The mobility values, on the other hand, do not reach a constant value at even the longest time delays, but decrease weakly following a power law. This weak, long-time decay of mobility is strikingly similar to the observed concentration dependence of mobility measured at fixed delay times shown in Fig. 7(a). Therefore, it may be related to a trap filling effect, since fewer carriers are extracted at longer time delays due to recombination. The observed Arrhenius-type activation of the mobility measured at long delay times, when the charge carriers occupy the deepest states, suggests that charge carrier hopping within an exponential distribution states is probed. A bimodal (intrinsic transport sites and an exponential distribution of traps) distribution within the MDMO-PPV/PCBM mixture has been previously suggested by Nelson *et al.* to explain the appearance of two different regimes of the recombination dynamics of the photogenerated charges.[15] The weak, power law concentration dependence of mobility seems to agree well with the results of Refs. 33–37, which predicted only a weak or negligible dependence of the mobility on the charge carrier concentration within the measured lower concentration range ($<10^{16}$ cm^3). We note, on the other hand, that the determination of the field dependent mobility using the photo-

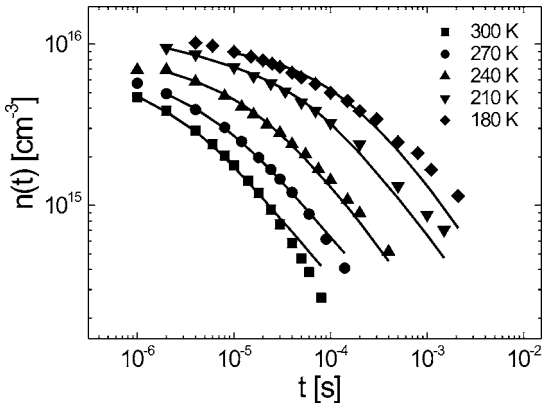

FIG. 11. Concentration decay of charge carriers fitted according to Eq. (9).

CELIV is prone to error when the field dependence of mobility is more pronounced. The complications in determination of the electric-field dependence of mobility at lower temperatures, together with the fact the electric-field dependence of mobility within only a rather limited range could be determined may be responsible for the observed deviations from the predicted $\log_{10}\mu(E=0)$ versus $(1000/T)^2$ straight line dependency as shown in the inset of Fig. 10.

Figures 4(a) and 4(b) clearly show that both the mobility and the recombination dynamics are time dependent in the studied MDMO-PPV/PCBM mixture. It is interesting to *directly* compare the measured time dependence of the mobility $\mu(t)$ in Fig. 4(a) with the time dependence of the bimolecular recombination coefficient $\beta(t)$ obtained from the concentration decay (Fig. 5). At high temperatures (>210 K) the power-law slopes of $\mu(t)$ are similar to that of $\beta(t)$, and it is therefore reasonable to assume that the bimolecular recombination coefficient is directly proportional to the mobility, i.e., $\beta(t)=B\mu(t)$, where B(V cm) is a constant. Using this relation, the concentration decay of charges [Eq. (4)] can be written as a function of the time-dependent mobility:

$$n(t)=\frac{n(0)}{1+n(0)B\int_0^t \mu(t)dt}. \tag{9}$$

The fits to the concentration decays at higher temperatures (>210 K) using Eq. (9) (the mobility values at all temperatures have been numerically integrated) are shown in Fig. 11. A reasonably good agreement is found, yielding $B=2\times10^{-7}$ V cm at 300 K, and slightly smaller values when the temperature is decreased. In the case of Langevin-type bimolecular charge carrier recombination,[21,29] $\beta=(e/\varepsilon\varepsilon_0)\mu$, and thus the proportionality constant B is directly given by $B=e/\varepsilon\varepsilon_0=6\times10^{-7}$ V cm (using $\varepsilon=3$ for the MDMO-PPV/PCBM blend). This value is relatively close to the value 2×10^{-7} V cm we obtained from the fit at 300 K, which suggests that Langevin-type bimolecular recombination is operative at room temperature and at the measured μs-ms time scale. We emphasize that the recombination is monitored at near zero electric-field conditions [flat bands due to application of the offset voltage (U_{offset}) prior charge extraction], yet the mobility is determined at a constantly changing, nonzero electric field. As it is shown in Fig. 9, the field dependence of mobility is weak at higher temperatures, but becomes increasingly important at lower temperatures. The electric field, which is calculated at the extraction maximum, depends on both space and time coordinate, therefore increases with increasing delay time ($t_{\max}$ shifts to longer times). Therefore, the pronounced electric-field dependence of mobility at lower temperature may affect the shape of the $\log_{10}\mu$ versus $\log_{10} t$ plots, and the proportionality between the measured $\mu(t)$ and $\beta(t)$ will no longer be valid.

B. Sign of the extracted carriers

If both charge carriers are mobile and their mobility is significantly different, two extraction peaks may be detected in the photo-CELIV experiments. In the studied MDMO-PPV:PCBM mixtures, only one extraction peak is observed at all applied delay times and applied voltages. This result suggests that the mobility of electrons and holes are very similar and the transport is nearly balanced. The mobility values measured by the photo-CELIV ($\sim\mu=10^{-4}$ cm^2 V^{-1} s^{-1}) and its electric field dependence are very similar to the hole mobility reported by Melzer *et al.* They also reported a one order of magnitude higher electron mobility, which we cannot confirm by our photo-CELIV measurements.[46] According to Eq. (1), the mobility is inversely proportional to the square of the time to reach the current extraction maximum $\mu\propto t_{\max}^{-2}$, therefore one order of magnitude higher mobility would mean an extraction peak that is shifted by a square root of 10 towards shorter time scales. Such rather smaller difference is maybe smeared out by the not negligible dispersion especially at shorter delay times.

The measured photo-CELIV mobility values, on the other hand, are one to two orders of magnitude higher than those measured using time-of-flight (ToF) photocurrent measurements.[47,48] A possible reason for the lower mobility in the thicker samples used in ToF may be related to the different morphology of the thicker films as it was also argued by Melzer *et al.*[46] Indeed, we observed that the mobility values determined using the photo-CELIV varies with film thickness especially when measured at longer time delays. Such differences in the morphology of MDMO-PPV:PCBM films have been previously observed using atomic force microscopy[49] and transmission electron microscopy.[50] The calculated apparent activation energy $\Delta E_\mu=120$ meV of the mobility measured by the photo-CELIV technique is smaller when compared to that of a pure MDMO-PPV investigated by the ToF technique ($\Delta=0.3-0.4$ eV), which further indicates that the activation energy possibly related to the morphology of the films is lowered in the mixture of MDMO-PPV with PCBM.

C. Implications to photovoltaic device performance

The number of extracted charge carriers clearly saturates with increasing light intensity indicating a concentration-

dependent recombination rate, which is in good agreement with the transient absorption (TA) measurements of Montanari *et al.*[4] The concentration decay of the extracted charge carriers, however, follows a hyperbolic decay characteristic of a bimolecular recombination in contrast to the power law decay of the polaron concentration as $p \propto t^{-\lambda}$ measured in the TA experiment. The difference may be related to the fact that only the reasonably mobile charge carriers are collected in the photo-CELIV technique, meanwhile the optical absorption of *all* the charge carriers including the immobile ones is monitored in the TA experiment. This has probably little effect on the concentration decay at room temperature, at which the number of unextracted charge carriers is minimal as indicated by the end of the pulse extraction current. It may, however, play an important role at lower temperatures, at which a non-negligible portion of the charge carriers remains in the device. The advantage of the photo-CELIV technique is that charge carrier recombination in operational devices is studied; therefore the measured mobility and lifetime values can be directly compared to the photovoltaic performance under operational conditions.

The product of $\mu\tau_B$ determined by the photo-CELIV technique at room temperature is $\sim 4 \times 10^{-10}$ cm^2 V^{-1}. The drift distance of the charge carriers using the above $\mu\tau_B$ value assuming an electric field of 5×10^4 V cm^{-1} is around $\sim l_d = 200$ nm. According to this result, the majority of the long-lived photogenerated charge carriers can be extracted in operational photovoltaic devices at short circuit conditions with active layer thickness not exceeding ~ 200 nm. This finding is consistent with frequent observations that the short circuit current is not limited by second order (bimolecular recombination) processes, but scales almost linearly with increasing incident light intensity.[51]

VI. CONCLUSIONS

Photo-CELIV transients at various delay times, light intensities and applied voltages have been recorded, and the charge carrier mobility and lifetime *simultaneously* studied. It is found that both the charge mobility and the recombination are time-dependent (dispersive) processes shortly after photoexcitation, which is attributed to the initial relaxation of the charge carriers towards the tail states of the density of states distribution. The results confirm that the recombination dynamics within the studied μs-ms time scale is a thermally activated process rather than a temperature independent tunneling. The obtained time-dependent mobility values are used to directly describe the recombination dynamics at higher temperatures. We have found that the recombination dynamics is nearly Langevin-type at room temperature, i.e., controlled by diffusion of the charge carriers towards each other. Deviations at lower temperatures, on the other hand, indicates that the determination of $\mu(t)$ from the extraction current transient maybe erratic when the electric-field dependence of the mobility is more pronounced. Finally, it is shown that although the charges are trapped on the longer time scales, their mobility is sufficiently high to be collected at external electrodes in typical bulk heterojunction solar cells.

ACKNOWLEDGMENTS

This work is supported by the European Commission within the framework of Research and Training Network (RTN) project EUROMAP (Contract No. HPRN-CT-2000-00127), and Academy of Finland through projects 206110 and 204884. We thank the group of Dirk Vanderzande for providing the MDMO-PPV. A. J. M. acknowledges financial support by the Japanese Society for the Promotion of Science (JSPS).

*Electronic address: amozer@molpro.mls.eng.osaka-u.ac.jp

[1] N. S. Sariciftci, D. Braun, C. Zhang, V. I. Srdanov, A. J. Heeger, G. Stucky, and F. Wudl, Appl. Phys. Lett. **62**, 585 (1993).

[2] R. H. Friend, R. W. Gymer, A. B. Holmes, J. H. Burroughes, R. N. Marks, C. Taliani, D. D. C. Bradley, D. A. Dos Santos, J. L. Brédas, M. Lögdlund, and W. R. Salaneck, Nature (London) **121**, 397 (1999).

[3] N. S. Sariciftci and A. J. Heeger, in *Handbook of Conductive Molecules and Polymers*, edited by H. S. Nalwa (John Wiley and Sons, New York, 1997).

[4] I. Montanari, A. F. Nogueira, J. Nelson, J. R. Durrant, C. Winder, M. A. Loi, N. S. Sariciftci, and C. J. Brabec, Appl. Phys. Lett. **81**, 3001 (2002).

[5] C. J. Brabec and N. S. Sariciftci, in *Semiconducting Polymers: Chemistry, Physics and Engineering*, edited by G. Hadziiannou and P. F. van Hutten (Wiley VCH, Weinheim, 2000).

[6] N. S. Sariciftci, L. Smilowitz, A. J. Heeger, and F. Wudl, Science **258**, 1474 (1992).

[7] C. J. Brabec, N. S. Sariciftci, and J. C. Hummelen, Adv. Funct. Mater. **11**, 15 (2001).

[8] N. A. Schultz, M. C. Scharber, C. J. Brabec, and N. S. Sariciftci, Phys. Rev. B **64**, 245210 (2001).

[9] M. C. Scharber, C. Winder, H. Neugebauer, and N. S. Sariciftci, Synth. Met. **141**, 109 (2004).

[10] C. Arndt, U. Zhokhavets, G. Bobsch, C. Winder, C. Lungenschmied, and N. S. Sariciftci, Thin Solid Films **451–452**, 60 (2004).

[11] A. F. Nogueira, I. Montanari, J. Nelson, J. R. Durrant, C. Winder, N. S. Sariciftci, and C. J. Brabec, J. Phys. Chem. B **107**, 1567 (2003).

[12] T. J. Savenije, J. E. Kroeze, M. M. Wienk, J. M. Kroon, and J. M. Warman, Phys. Rev. B **69**, 155205 (2004).

[13] N. F. Mott and R. A. Gurney, *Electronic Processes in Ionic Crystals* (Dover Publications, New York, 1964).

[14] A. J. Mozer, N. S. Sariciftci, L. Lutsen, D. Vanderzande, R. Österbacka, M. Westerling, and G. Juška, Appl. Phys. Lett. **86**, 112104 (2005).

[15] J. Nelson, Phys. Rev. B **67**, 155209 (2003).

[16] J. Nelson, S. A. Choulis, and J. R. Durrant, Thin Solid Films **451-452**, 508 (2004).

[17] R. Österbacka, A. Pivrikas, G. Juška, K. Genevičius, K. Arlauskas, and H. Stubb, Curr. Appl. Phys. **4**, 534 (2004).

[18] G. Juška, K. Arlauskas, M. Viliūnas, and J. Kočka, Phys. Rev. Lett. **84**, 4946 (2000).
[19] G. Juška, M. Viliunas, K. Arlauskas, N. Nekrašas, N. Wyrsch, and L. Feitknecht, J. Appl. Phys. **89**, 4971 (2001).
[20] A. J. Mozer, P. Denk, M. C. Scharber, H. Neugebauer, N. S. Sariciftci, P. Wagner, L. Lutsen, and D. Vanderzande, J. Phys. Chem. B **108**, 5235 (2004).
[21] U. Albrecht and H. Bässler, Phys. Status Solidi B **191**, 455 (1995).
[22] H. Bässler, Phys. Status Solidi B **107**, 9 (1981).
[23] H. Bässler, Phys. Status Solidi B **175**, 15 (1993). The equation $t_{rel}/t_0=10\ \exp[-1.07\ (\sigma/kT)^2]$ appeared with the incorrect minus sign in the exponent. The correct equation reads $t_{rel}/t_0=10\ \exp[1.07\ (\sigma/kT)^2]$, (private communication, H. Bässler).
[24] S. V. Novikov, D. H. Dunlap, V. M. Kenkre, P. E. Parris, and A. V. Vannikov, Phys. Rev. Lett. **81**, 4472 (1998).
[25] V. I. Arkhipov, P. Heremans, E. V. Emelianova, G. J. Adriaenssens, and H. Bässler, J. Phys.: Condens. Matter **14**, 9899 (2002).
[26] B. Movaghar, M. Grünewald, B. Ries, H. Bässler, and D. Würtz, Phys. Rev. B **33**, 5545 (1986).
[27] M. V. Smoluchowski, Z. Phys. Chem., Stoechiom. Verwandtschaftsl. **92**, 129 (1917).
[28] T. R. Waite, Phys. Rev. **107**, 463 (1957).
[29] M. Pope and C. E. Swenberg, *Electronic Processes in Organic Crystals and Polymers*, 2nd ed. (Oxford University Press, New York, 1999).
[30] M. Scheidler, B. Cleve, H. Bässler, and P. Thomas, Chem. Phys. Lett. **225**, 431 (1994).
[31] M. Grünewald, B. Movaghar, B. Pohlmann, and D. Würtz, Phys. Rev. B **32**, 8191 (1985).
[32] G. Juška, N. Nekrasas, K. Genevičius, J. Stuchlik, and J. Kočka, Thin Solid Films **451-452**, 290 (2004).
[33] Y. Roichman and N. Tessler, Appl. Phys. Lett. **80**, 1948 (2002).
[34] V. I. Arkhipov, P. Heremans, E. V. Emelianova, G. J. Adriaenssens, and H. Bässler, Appl. Phys. Lett. **82**, 3245 (2003).
[35] C. Tanase, E. J. Meier, P. W. M. Blom, and D. M. de Leeuw, Phys. Rev. Lett. **91**, 216601 (2003).
[36] C. Tanase, P. W. M. Blom, and D. M. de Leeuw, Phys. Rev. B **70**, 193202 (2004).
[37] V. I. Arkhipov, P. Heremans, E. V. Emelianova, and H. Bässler, Phys. Rev. B **71**, 045214 (2005).
[38] P. W. M. Blom, M. J. M. de Jong, and J. J. M. Vleggaar, Appl. Phys. Lett. **68**, 3308 (1996).
[39] G. Juška, K. Genevičius, K. Arlauskas, R. Österbacka, and H. Stubb, Phys. Rev. B **65**, 233208 (2002).
[40] V. I. Arkhipov, E. V. Emelianova, and H. Bässler, Philos. Mag. B **81**, 985 (2001).
[41] I. I. Fishchuk, D. Hertel, H. Bässler, and A. Kadashchuk, Phys. Rev. B **65**, 125201 (2002).
[42] V. I. Arkhipov, E. V. Emelianova, and G. J. Adriaenssens, Phys. Rev. B **64**, 125125 (2001).
[43] A. Miller and E. Abrahams, Phys. Rev. **120**, 745 (1960).
[44] L. Pautmeier, R. Richert, and H. Bässler, Philos. Mag. Lett. **59**, 325 (1989).
[45] A. J. Mozer, N. S. Sariciftci, A. Pivrikas, R. Österbacka, G. Juška, L. Brassat, and H. Bässler, Phys. Rev. B **71**, 035214 (2005).
[46] C. Melzer, E. J. Koop, V. D. Mihailetci, and P. W. M. Blom, Adv. Funct. Mater. **14**, 865 (2004).
[47] S. A. Choulis, J. Nelson, Y. Kim, D. Poplavskyy, T. Kreouzis, J. R. Durrant, and D. D. C. Bradley, Appl. Phys. Lett. **83**, 3812 (2003).
[48] S. A. Choulis, J. Nelson, S. M. Tuladhar, S. Cook, Y. Kim, J. R. Durrant, and D. D. C. Bradley, Macromol. Symp. **205**, 1 (2004).
[49] H. Hoppe, M. Niggemann, C. Winder, J. Kraut, R. Hiesgen, A. Hinsch, D. Meissner, and N. S. Sariciftci, Adv. Funct. Mater. **14**, 1005 (2004).
[50] T. Martens, J. D'Haen, T. Munters, Z. Beelen, L. Goris, J. Manca, M. D'Olieslaeger, D. Vanderzande, L. De Schepper, and R. Andriessen, Synth. Met. **138**, 243 (2003).
[51] I. Riedel, J. Parisi, V. Dyakonov, L. Lutsen, D. Vanderzande, and J. C. Hummelen, Adv. Funct. Mater. **14**, 38 (2004).